JEMAT 2023, Vol 11, No 1, 52-61
https://doi.org/10.54987/jemat.v11i1.884

HIBISCUS PUBLISHER

JOURNAL OF ENVIRONMENTAL MICROBIOLOGY AND TOXICOLOGY

Website: http://journal.hibiscuspublisher.com/index.php/JEMAT/index

Adsorption of Sodium Dodecyl Sulfate onto Activated Coconut Shell-Based Adsorbent: Isothermal Remodelling

Shakirah Abdul Wahab Sha'arani [1], Nur Adeela Yasid[1], Mohd Izuan Effendi Halmi[2], Ahmad Razi Othman[3] and Mohd Yunus Shukor[1]*

[1]Department of Biochemistry, Faculty of Biotechnology and Biomolecular Sciences, Universiti Putra Malaysia, 43400 UPM Serdang, Selangor, Malaysia.
[2]Department of Soil Management, Faculty of Agriculture Universiti Putra Malaysia, 43400 UPM Serdang, Selangor, Malaysia.
[3]Department of Chemical Engineering, Faculty of Engineering and Built Environment, Universiti Kebangsaan Malaysia, 43600 UKM Bangi, Selangor, Malaysia.

*Corresponding author:
Mohd Yunus Shukor,
Department of Biochemistry,
Faculty of Biotechnology and Biomolecular Sciences,
Universiti Putra Malaysia,
43400 UPM Serdang,
Selangor,
Malaysia.
Email: mohdyunus@upm.edu.my

HISTORY

Received: 15th May 2023
Received in revised form: 5th July 2023
Accepted: 30th July 2023

KEYWORDS

SDS
activated carbon
coconut shell
isotherms
Moreau

ABSTRACT

A remodelling evaluation was conducted on the sorption isotherm data for SDS adsorption onto activated coconut shell using nonlinear regression. A total of nineteen models, including BET, Brouers-Sotolongo, Dubinin-Radushkevich, Fowler-Guggenheim, Freundlich, Fritz-Schlunder III, Hill, Henry, Jovanovic, Khan, Langmuir, Moreau, Radke-Prausnitz, Redlich-Peterson, Sips, Temkin, Toth, Unilan, and Vieth-Sladek, were employed to determine the best fit through non-linear regression. All models were found to exhibit good fits to the data, except for the Fowler-Guggenheim, Henry and Dubinin-Radushkevich models. Statistical analysis based on error function assessments, including accuracy factor (AF), bias factor (BF), root-mean-square error (RMSE), adjusted coefficient of determination (adjR^2), Bayesian Information Criterion (BIC), corrected AICc (Akaike Information Criterion), and Hannan-Quinn Criterion (HQC), revealed that the best performance was achieved by the Moreau model followed by (descending order) Unilan, Redlich-Peterson, Fritz-Schlunder III, Toth, and Langmuir. The maximum adsorption capacity estimates given by the Moreau and Langmuir models were better in line with experimental findings. The value of the maximum monolayer adsorption capacity for SDS binding to activated coconut shell according to the Langmuir's parameter q_{mL} was 81.93 mg g^{-1} (95% Confidence interval from 76.422 to 87.440), while b_L (L mg^{-1}), the Langmuir model constants was 0.10 L mg^{-1} (95% C.I. from 0.070 to 0.133). The value of the maximum monolayer adsorption capacity for SDS binding to activated coconut shell according to the Moreau's parameter q_{mM} was 90.82 mg g^{-1} (95% Confidence interval from 76.336 to 105.303), while b (L mg^{-1}), the Moreau's model constant was 0.15 L mg^{-1} (95% C.I. from 0.089 to 0.203) and l, another Moreau's dimensionless constant was 0.3 (95% C.I. from -0.049 to 0.646).

INTRODUCTION

Surfactants are widely utilized in both household and industrial settings owing to their typical physicochemical properties, particularly their surface activity. These molecules consist of a hydrophilic head and a hydrophobic tail, which give them amphiphilic properties [1]. Surfactants are categorized into four types based on their chemical structure: cationic, anionic, nonionic, and zwitter ionic [2]. Anionic surfactants serve as pivotal components in various products such as detergents, toothpaste, shampoo, pesticides, textile paints and personal care items [3,4]. Moreover, they find application in diverse fields including soil remediation, enhanced oil recovery, dispersion, emulsion polymers, deinking, ore flotation and cutting oils [5]. Because of their extensive use and versatility, surfactants frequently end up in both industrial and domestic wastewater, as they might not be fully utilized in their intended applications. Some of the discharged surfactants may undergo natural degradation. However, reliance solely on biodegradation or natural breakdown might not suffice, especially when surfactants are present in high concentrations [6]. Residual surfactants, particularly the anionic vari-

ants, can adversely affect aquatic microorganisms and ecosystems in water bodies. Additionally, if these surfactants enter the food chain, they can also pose risks to humans [7]. Moreover, the presence of surfactants can impact the effectiveness of wastewater treatment plants [8]. For instance, surfactants can influence sludge dewatering characteristics and enhance the solubility of organic compounds, thus affecting treatment efficacy [9]. Therefore, it is crucial to devise an efficient treatment method for removing surfactants, as attempted in the current study, focusing on a specific case of SDS.

SDS, a fundamental and significant anionic surfactant, finds extensive application in detergents, shampoos, and cosmetics. SDS has been linked to symptoms like depression, difficulty breathing, and diarrhea in both humans and animals [10]. SDS also induces acute and chronic toxicity in fish [11]. Surfactants elevate the solubility of organic compounds in water, potentially increasing the carcinogenicity and risk of dermatitis, as documented in literature [7,12]. Given the environmental and health concerns, the acceptable limits for surfactants in water intended for domestic use are set at 1 mg/L, and even lower at 0.5 mg/L for potable water [13]. These stringent regulations underscore the necessity for treating wastewater containing surfactants. Thus, the significance of the present study on SDS removal is highlighted.

Several methods, including adsorption [2,4,5,13], ultra-filtration [14,15], biodegradation [10] and advanced oxidation [9], are commonly used for wastewater treatment. Among these methods, adsorptive separation stands out due to its versatility in fine-tuning adsorbent performance, the potential for synthesizing adsorbents from biomass or waste materials, and its feasibility for large-scale continuous operation. The synthesis of adsorbents from various materials, including biomass waste such as coconut shell [5,16], wood, wood stalks, sawdust, sugarcane bagasse, seeds, seed hulls, jackfruit peels, coffee beans [17–21], microalgae, etc., has been extensively documented in the literature. In previous study [16], the adsorptive separation of sodium dodecyl benzene sulfonate (SDBS) using a biosorbent derived from coconut shells was investigated, demonstrating its efficacy. The current research extends the work by applying the same biosorbent (PAACS-I) to the adsorptive separation of SDS [5], another significant anionic surfactant. The influence of various operating parameters on the SDS removal efficiency was examined, conducting a comprehensive analysis of kinetics and thermodynamics to elucidate the adsorption mechanism and heat effects.

Gaining a full understanding of the biosorption process in distinct species requires a careful examination of the kinetics and isotherms. The data in question is intrinsically nonlinear, although scientific publications frequently depict it as though it were linear. Nevertheless, the error structure linked to essentially nonlinear data is changed during the linearization process. One problem with this method is that it makes the modified data's residuals seem less likely to follow a normal distribution. [22]. Consequently, it gets increasingly difficult to put a number on uncertainty, which is typically shown as a 95% confidence range. The purpose of this research is to review and reevaluate an earlier paper on SDS sorption upon AC shroud [5], which employed linear regression to derive the best-fitting models.

METHOD

Data acquisition and fitting

Figure 9 data (323 K) from a previously published study [5] was digitized using the freeware Webplotdigitizer 2.5 [23]. The program's digitization capabilities have garnered accolades for their reliability [24]. Following that, Curve-Expert Professional (Version 2.6.5, copyright Daniel Hyams), a program for curve fitting, was used to perform nonlinear regression on the data. The software package MATLAB (Mathworks, Massachusetts, USA) was used to resolve the implicit equations.

Isotherms

As the value of the data points is very small, only models having parameters of up to three were considered to prevent overfitting.

Table 1. Mathematical models that were used in modelling data.

Isotherm	p	Formula	Ref.
Henry's law	1	$q_e = HC_e$	[25]
Langmuir	2	$q_e = \frac{q_{mL} b_L C_e}{1 + b_L C_e}$	[26]
Jovanovic	2	$q_e = q_{mJ}(1 - e^{-K_J C_e})$	[27]
Freundlich	2	$q_e = K_F C_e^{\frac{1}{n_F}}$	[28]
Dubinin-Radushkevich	2	Incorrect form $q_e = q_{mDR} exp\left\{-K_{DR}\left[RTln\left(1+\frac{1}{C_e}\right)\right]^2\right\}$	[29,30]
		correct form $q_e = q_{mDR} exp\left\{-K_{DR}\left[RTln\left(\left(\frac{C_s}{C_e}\right)\right)\right]^2\right\}$	[31,32]
Temkin	3	$q_e = \frac{RT}{b_T}\{ln(a_T C_e)\}$	[33,34]
Redlich-Peterson	3	$q_e = \frac{K_{RP1} C_e}{1 + K_{RP2} C_e^{\beta_{RP}}}$	[35]
Sips	3	$q_e = \frac{K_s q_{mS} C_e^{\frac{1}{n_S}}}{1 + K_S C_e^{\frac{1}{n_S}}}$	[36]
Toth	3	$q_e = \frac{q_{mT} C_e}{\left(K_T + C_e^{n_T}\right)^{n_T}}$	[37]
Hill	3	$q_e = \frac{q_{mH} C_e^{n_H}}{K_H + C_e^{n_H}}$	[38]
Khan	3	$q_e = \frac{q_{mK} b_K C_e}{(1 + b_K C_e)^{a_K}}$	[39]
BET	3	$q_e = \frac{q_{mBET} \alpha_{BET} C_e}{(1 - \beta_{BET} C_e)(1 - \beta_{BET} C_e + \alpha_{BET} C_e)}$	[40]
Vieth-Sladek	3	$q_e = \frac{q_{mVS} b_{VS} C_e}{(1 + b_{VS} C_e)^{n_{VS}}}$	[41]
Radke-Prausnitz	3	$q_e = \frac{A_{RP} B_{RP} C_e^{\beta}}{A_{RP} + B_{RP} C_e^{\beta - 1}}$	[42–44]
Brouers–Sotolongo	3	$q_e = q_{mBS}\left[1 - \left(1 + (0.5)\left(\frac{t}{\tau}\right)^{\alpha}\right)^{-2}\right]$	[45,46]
Fritz-Schlunder-III	3	$q_e = \frac{q_{mFS} K_{FS} C_e}{1 + K_{FS} C_e^{n_{FS}}}$	[47]
Fowler-Guggenheim*	3	$q_e = q_{mFG} \frac{K_L C_e e^{\frac{\alpha q_e}{q_{mFG}}}}{1 + K_L C_e e^{\frac{\alpha q_e}{q_{mFG}}}}$	[48]
Moreau	3	$q_e = q_{mM} \frac{bC_e + lb^2 {C_e}^2}{1 + 2bC_e + lb^2 {C_e}^2}$	[49]
Unilan	3	$q_e = \frac{q_{mU}}{2b_U} ln\left(\frac{a_U + C_e e^{b_U}}{a_U + C_e e^{-b_U}}\right)$	[50]
Baudu	4	$q_e = \frac{q_{mB} b_B C_e^{(1+x+y)}}{1 + b_B C_e^{(1+x)}}$	[51]
Marczewski-Jaroniec	4	$q_e = q_{mMJ}\left(\frac{(K_{MJ} C_e)^{n_{MJ}}}{1 + (K_{MJ} C_e)^{n_{MJ}}}\right)^{\frac{m_{MJ}}{n_{MJ}}}$	[47]
Fritz-Schlunder-IV	4	$q_e = \frac{A_{FS} C_e^{a_{FS}}}{1 + B_{FS} C_e^{b_{FS}}}$	[52]
Weber-van Vliet*	4	$C_e = P_1 q_e^{\left(P_2 q_e^{P_3} + P_4\right)}$	

Note *Implicit equation or function.

Statistical analysis

The following statistical discriminatory tests were utilized in this study: HQ, BF, AF, RMSE, adjusted coefficient of determination (R^2), corrected Akaike Information Criterion (AICc), BIC, and Hannan and Quinn's Criterion (AIC). The root-mean-squared error (RMSE) was calculated using Eqn. 1, which indicates that in most cases, a reduced RMSE is obtained with fewer parameters. Where n is the total number of observations, Obi and Pdi are the predicted and observed values, and p is the total number of parameters utilized in this context [22].

$$RMSE = \sqrt{\frac{\sum_{i=1}^{n}(Pd_i - Ob_i)^2}{n-p}} \quad \text{(Eqn. 1)}$$

The modified R^2 is utilized to overcome the limitation that R^2, which stands for the coefficient of determination, does not take into account the total number of parameters in a model. The total variance of the y-variable is represented by S^2_y in the equation (Equations 2 and 3), while RMS refers to the Residual Mean Square.

$$Bias\ factor = 10\left(\sum_{i=1}^{n} log\frac{(Pd_i/Ob_i)}{n}\right) \quad \text{(Eqn. 2)}$$

$$Accuracy\ factor = 10\left(\sum_{i=1}^{n} log\frac{|(Pd_i/Ob_i)|}{n}\right) \quad \text{(Eqn. 3)}$$

In the AICc equation, p is the number of parameters and n is the number of data points, and the AICc is derived accordingly. Data sets with many parameters but few values are best handled by applying the updated Akaike information criterion (AICc). [53]. It is more probable that a model is correct if its AICc score is lower [53]. The AIC's (Akaike Information Criterion) basis is information theory. It finds a happy medium between a model's complexity and its goodness of fit [54].

$$AICc = 2p + n\ln\left(\frac{RSS}{n}\right) + \frac{2(p+1)+2(p+2)}{n-p-2} \quad \text{(Eqn. 4)}$$

In addition to AICc, the Bayesian Information Criterion (BIC) (Equation 5) is another information-theory-based statistical tool. This error function penalizes parameter count more harshly than AIC [55].

$$BIC = n\ln\left(\frac{RSS}{n}\right) + k\ln(n) \quad \text{(Eqn. 5)}$$

Equation 6 represents the Hannan-Quinn information criterion (HQC), an additional information theory-based method for error functions. The HQC is more reliable than the AIC due to the inclusion of the ln n element in the calculation [53].

$$HQC = nIn\left(\frac{RSS}{n}\right) + 2k\ln(\ln n) \quad \text{(Eqn. 6)}$$

Two further error function analyses extracted from Ross's research are the Accuracy Factor (AF) and the Bias Factor (BF) [53]. Rather than penalizing models based on their parameter counts, these error functions empirically assess their goodness-of-fit (**Equations 7** and **8**).

$$Adjusted\ (R^2) = 1 - \frac{RMS}{S_Y^2} \quad \text{(Eqn. 7)}$$

$$Adjusted\ (R^2) = 1 - \frac{(1-R^2)(n-1)}{(n-p-1)} \quad \text{(Eqn. 8)}$$

A typical error function utilized in much isotherm research is Marquardt's percent standard deviation (MPSD). Depending on the number of degrees of freedom in the system, the function takes on a shape similar to a geometric mean error distribution [56]. Among the first to use this error function in the adsorption field is [57] and the McKay group first proposed the official name for the error function, which is MPSD (Equation 9) [58].

$$MPSD = 100\sqrt{\frac{1}{n-p}\sum_{i=1}^{n}\left(\frac{Ob_i - Pd_i}{Ob_i}\right)^2} \quad \text{(Eqn. 9)}$$

in which n is the total number of experimental data points, p is the total number of parameters, *Obi* is the set of experimental data points, and *Pdi* is the value that the model predicts.

RESULTS AND DISCUSSION

Several models were applied to the equilibrium data given in [5] by non-linear regression. Importantly, as shown in **Figs.** 1–18, all of these models showed good data fits with the exception of the Henry, Dubinin–Radushkevich models. There was no convergence in the Fowler-Guggenheim model. Among several assessment metrics, the Moreau isotherm model stood out as the top performer. These metrics included having the shortest RMSE, adjusted R^2, AF, and BF values close to one, as well as the lowest values for Bayesian Factor (BF), MPSD, and AICc values. Nevertheless, the Langmuir model emerged as the top performer when AICc was utilized as the only error function. Moreau, Unilan, Redlich-Peterson, Fritz-Schlunder III, Toth, and Langmuir were the top models in descending order according to the majority error function analysis.

The Unilan, Redlich-Peterson, Fritz-Schlunder III, and Toth models all performed well, but their maximum adsorption capacities were very different from the experimental values, and the wide 95% confidence interval demonstrated that they were not a good fit. The small sample size is probably to blame for this disparity. On the other hand, the maximum adsorption capacity estimates given by the Moreau and Langmuir models were better in line with experimental findings. Nonlinear regression provides more accurate results than linear regression, which was utilized in the original publication—which only presented the linearized forms of the Langmuir, Temkin, Dubinin-Radushkevich, and Freundlich models—because many models fit the bentonite data well.

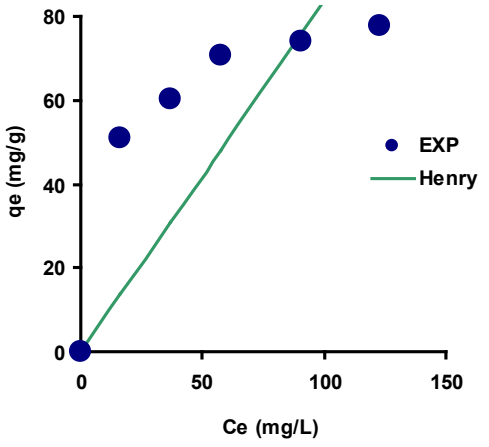

.

Fig. 1. SDS adsorption isotherm onto activated coconut shell as modelled using the Henry model.

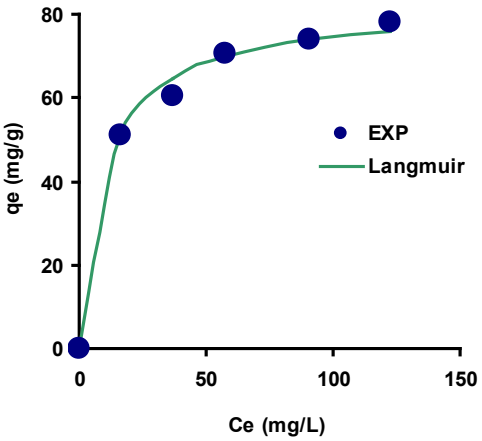

Fig. 2. SDS adsorption isotherm onto activated coconut shell as modelled using the Langmuir isotherm model.

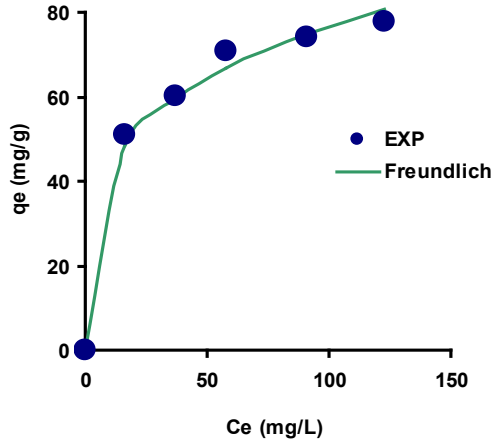

Fig. 3. SDS adsorption isotherm onto activated coconut shell as modelled using the Freundlich isotherm model.

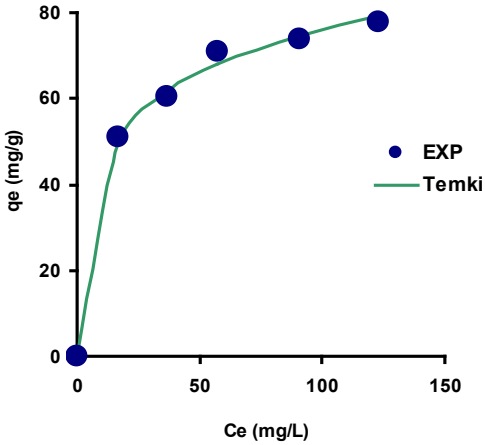

Fig. 4. SDS adsorption isotherm onto activated coconut shell as modelled using the Temkin isotherm model.

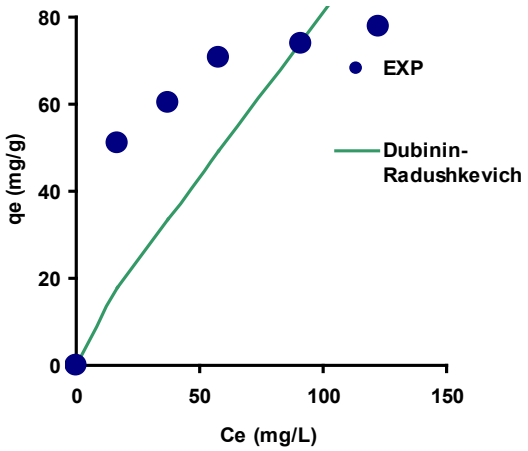

Fig. 5. SDS adsorption isotherm onto activated coconut shell as modelled using the Dubinin-Radushkevich isotherm model.

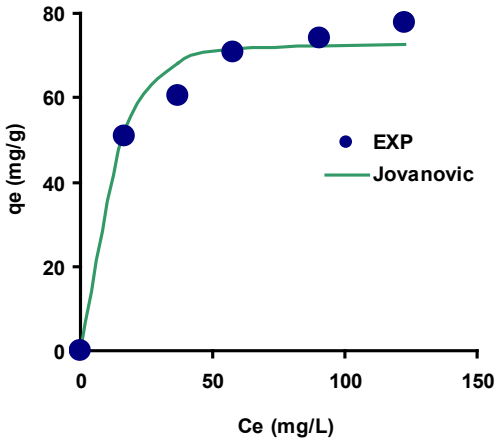

Fig. 6. SDS adsorption isotherm onto activated coconut shell as modelled using the Jovanovic isotherm model.

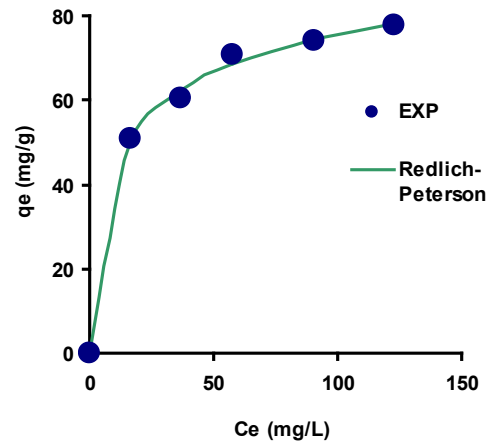

Fig. 7. SDS adsorption isotherm onto activated coconut shell as modelled using the Redlich-Peterson isotherm model.

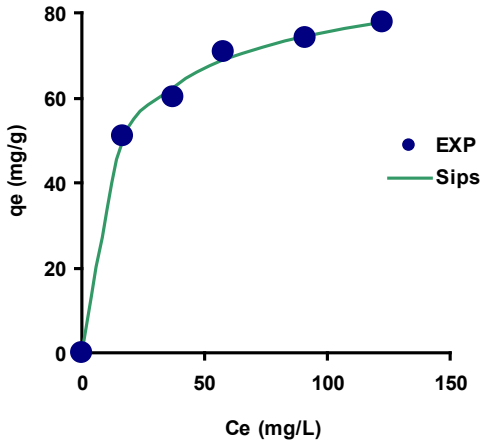

Fig. 8. SDS adsorption isotherm onto activated coconut shell as modelled using the Sips isotherm model.

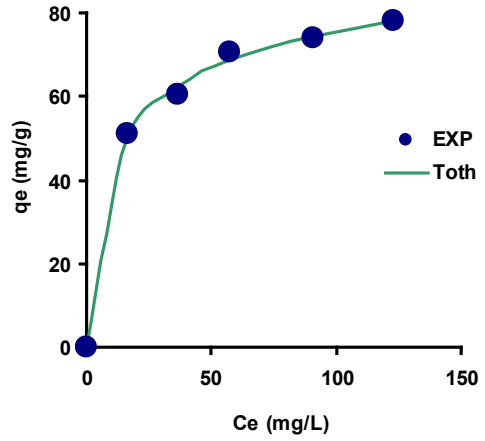

Fig. 9. SDS adsorption isotherm onto activated coconut shell as modelled using the Toth isotherm model.

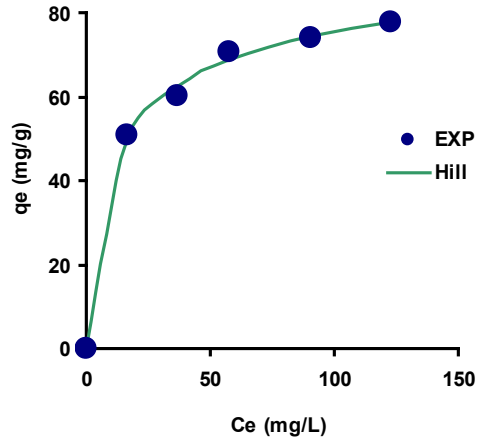

Fig. 10. SDS adsorption isotherm onto activated coconut shell as modelled using the Hill isotherm model.

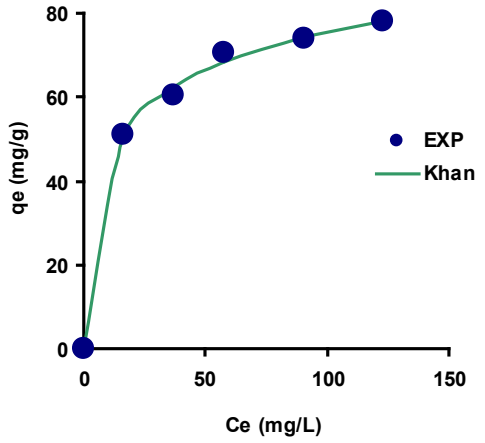

Fig. 11. SDS adsorption isotherm onto activated coconut shell as modelled using the Khan isotherm model.

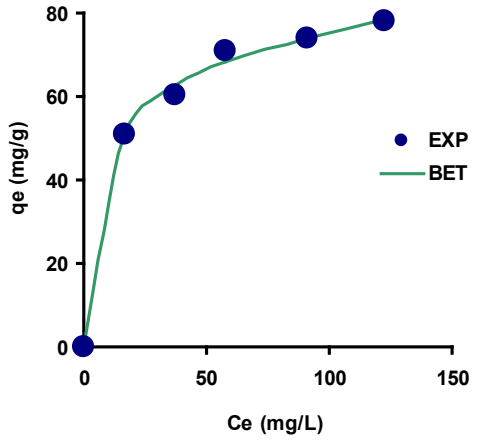

Fig. 12. SDS adsorption isotherm onto activated coconut shell as modelled using the BET isotherm model.

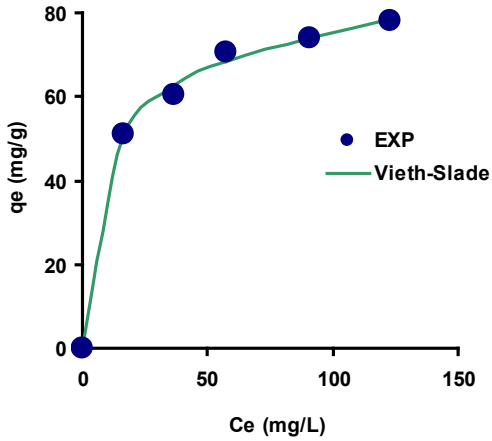

Fig. 13. SDS adsorption isotherm onto activated coconut shell as modelled using the Vieth-Sladek isotherm model.

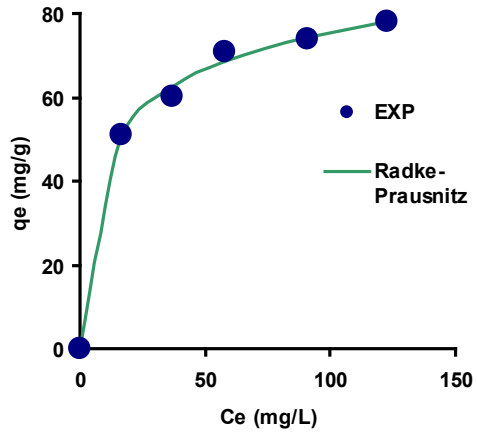

Fig. 14. SDS adsorption isotherm onto activated coconut shell as modelled using the Radke-Prausnitz isotherm model.

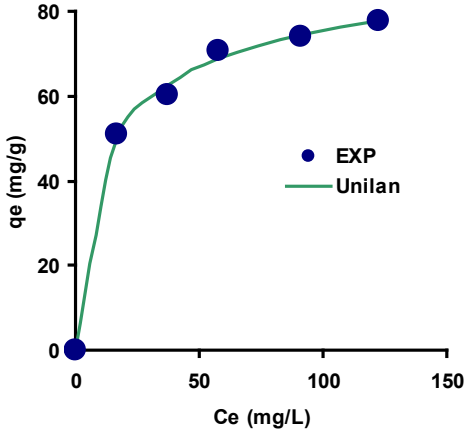

Fig. 17. SDS adsorption isotherm onto activated coconut shell as modelled using the Unilan isotherm model.

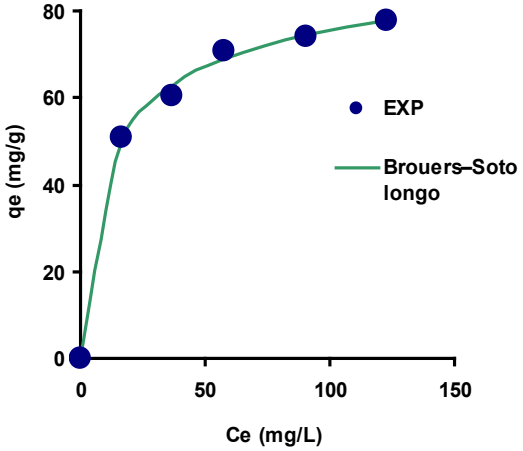

Fig. 15. SDS adsorption isotherm onto activated coconut shell as modelled using the Brouers-Sotolongo isotherm model.

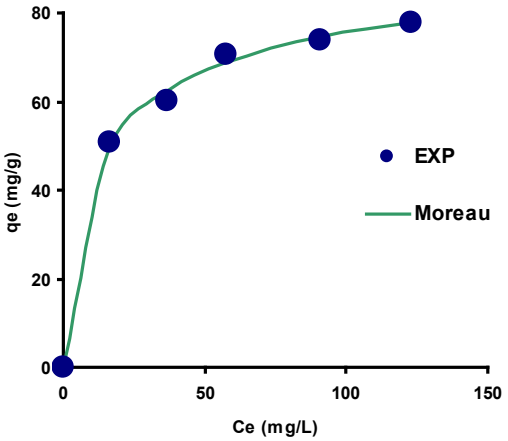

Fig. 18. SDS adsorption isotherm onto activated coconut shell as modelled using the Moreau isotherm model.

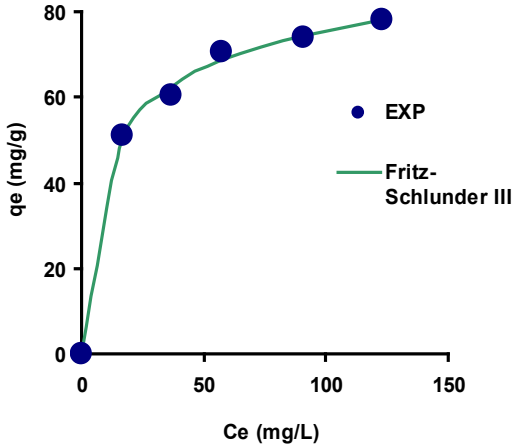

Fig. 16. SDS adsorption isotherm onto activated coconut shell as modelled using the Fritz-Schlunder III isotherm model.

Table 2. Error function analysis for the fitting of the isotherm of SDS onto activated coconut shell.

Model	MPSD	RMSE	adR2	AICc	BIC	HQC	BF	AF
Moreau	157.5	1.58	1.00	36.45	8.28	6.44	1.00	1.01
Unilan	158.8	1.59	1.00	36.56	8.40	6.55	1.00	1.01
Redlich-Peterson	159.7	1.60	1.00	36.63	8.47	6.63	1.00	1.01
Fritz-Schlunder III	159.7	1.60	1.00	36.63	8.47	6.63	1.00	1.01
Toth	159.9	1.60	1.00	36.66	8.49	6.65	1.00	1.01
Khan	160.3	1.60	1.00	36.69	8.52	6.68	1.00	1.01
Radke-Prausnitz	160.3	1.60	1.00	36.69	8.52	6.68	1.00	1.01
Hill	160.7	1.61	1.00	36.73	8.56	6.72	1.00	1.02
Sips	160.7	1.61	1.00	36.73	8.56	6.72	1.00	1.02
Brouers–Sotolongo	162.0	1.62	1.00	36.84	8.68	6.84	1.00	1.02
Vieth-Sladek	174.2	1.74	0.99	37.85	9.69	7.85	1.00	1.01
BET	177.9	1.78	0.99	38.15	9.98	8.14	1.00	1.01
Marczewski	183.3	1.83	0.99	80.55	10.34	7.88	1.00	1.01
Baudu	184.2	1.84	0.99	80.62	10.40	7.94	1.00	1.01
Fritz-Schlunder IV	184.2	1.84	0.99	80.62	10.40	7.94	1.00	1.01
Weber-van Vliet	187.6	1.88	0.99	80.88	10.66	8.21	1.00	1.02
Temkin	190.9	1.91	0.99	39.13	10.97	9.13	1.00	1.02
Langmuir	240.9	2.41	0.99	27.95	13.84	12.61	1.00	1.03
Freundlich	312.4	3.12	0.98	31.59	17.48	16.25	1.01	1.04
Jovanovic	525.2	5.25	0.96	38.87	24.76	23.53	0.98	1.07
Dubinin-Radushkevich	2577.8	25.78	0.39	61.14	47.03	45.80	0.22	4.86
Henry	2643.2	26.43	0.43	53.77	46.71	46.10	0.57	1.92
Fowler-Guggenheim	n.a.	n.a.	n.a.	n.a.	n.a.	n.a.	n.a.	n.a.

Note:
RMSE Root mean Square Error
adR^2 Adjusted Coefficient of determination
p no of parameters
AF Accuracy factor
BF Bias factor
BIC Bayesian Information Criterion
AICc Adjusted Akaike Information Criterion
HQC Hannan–Quinn information criterion

Moreau

Interactions between adsorbates occur on a homogenous adsorbent surface, as described by the Moreau isotherm model [59], furthermore, the Ruthven model, which was created for zeolite adsorption, is very similar to this one [60]. Proteins adsorb to polymer surfaces by a complex web of interactions, some of which include hydrogen bonding, van der Waals forces, and hydrophobic effects. Taking into account the heterogeneity and interaction among adsorbed proteins, the Moreau isotherm was determined to be the most effective model for the adsorption process [61]. The value of the maximum monolayer adsorption capacity for SDS binding to activated coconut shell according to the Moreau's parameter q_{mM} was 90.82 mg g-1 (95% Confidence interval from 76.336 to 105.303), while b (L mg^{-1}), the Moreau's model constant was 0.15 L mg^{-1} (95% C.I. from 0.089 to 0.203) and l, another Moreau's dimensionless constant was 0.3 (95% C.I. from -0.049 to 0.646).

Unilan (Unilin) model

Among the empirical correlations proposed for use in equilibrium data analysis in the book by Valenzuela and Myers is Unilan. Some publications also use the name Unilin when UniLan is more appropriate. An acronym for "Uniform distribution and Langmuir local" isotherm, UniLan describes this design. Assuming a surface that is defined patch-wise, the Unilan equation states that the local Langmuir equation is applicable to each patch [62]. The Unilan equilibrium constant (a_U) and model exponent (b_U) are used in this isotherm, while q_{mU} (mg g^{-1}) is the maximal monolayer adsorption capacity predicted by the isotherm.

The variability of the system is described by b_U. The more this parameter's value increases, the more diverse the system gets. The UniLan equation is transformed into the classical Langmuir equation when $b_U = 0$ in this limit, which also happens when the value for the range of energy distribution becomes zero [63]. The result of the remodeling exercise, however, did not conform to the observed experimental q_m value of about 90 mg g^{-1} (**Table 3**).

Langmuir isotherm

There is a continuum between empirical and mechanistic isotherm models; the Langmuir isotherm is definitely in the former. On the assumption of structural homogeneity in the adsorbent and equal energy for all adsorption sites, this model postulates that adsorption occurs as a uniform monolayer on the adsorbent surface [64]. Because intermolecular interactions decrease exponentially with increasing distance, it predicts that a monolayer will form on the outer adsorbent surface. The linearization of the relationship and the assumption of a constant monolayer adsorption capacity are both brought about by this. That Henry's model holds true for both extremely dilute and concentrated solute concentrations is another important finding [65].

The Freundlich and Langmuir models are two of the most popular choices for sorption research. The nonlinear regression method was able to get parameter estimates that were quite similar to the original study's, but it couldn't give a 95% confidence interval. The value of the maximum monolayer adsorption capacity for SDS binding to activated coconut shell according to the Langmuir's parameter q_{mL} was 81.93 mg g-1 (95% Confidence interval from 76.422 to 87.440), while b_L (L mg^{-1}), the Langmuir model constants was 0.10 L mg^{-1} (95% C.I. from 0.070 to 0.133). These values are very similar to the reported linear regressed values in the original publication for q_{mL} and b_L values at 90.9 mg g-1 and 0.09 L mg^{-1}, respectively [5] (**Table 4**).

Toth isotherm

The Toth isotherm model serves as an equation used to explain adsorption processes, on surfaces with variations. It is crafted to address differences from the Langmuir isotherm, which assumes adsorption sites and single layer adsorption. The Toth isotherm provides flexibility in describing adhesion behaviors that differ from the Langmuir model by accommodating both high concentrations of adsorbate. By incorporating the parameter n_T it accommodates surface diversity simplifying to match the Langmuir isotherm. In fields such, as engineering, wastewater treatment and material science the process of adsorption involves capturing pollutants, dyes, heavy metals and other impurities on different materials like activated carbon, clays and biochar.

The Toth isotherm is preferred over models as it fits data better especially in cases of varied adsorption environments. This model can handle a range of adsorption scenarios due to its parameters. However it is more intricate than models like Langmuir or Freundlich as it requires estimating parameters. The Toth isotherm serves as an adaptable tool for explaining adsorption on surfaces with greater precision for systems that deviate from simpler model assumptions. The Toth isotherm was found as the best isotherm for the adsorption of two organic dyes (alizarin red S and phenol red) on mesoporous silica and hybrid gels [66], the adsorption of the red, yellow, and mustard yellow acid dyes onto granular activated carbon [67] adsorption of CO_2 using biochar and KOH and $ZnCl_2$ activated carbons derived from pine sawdust [68] and adsorption of ammonia onto an activated carbon [69].

Redlich-Peterson isotherm

The Redlich-Peterson isotherm is a widely used model in adsorption studies that combines elements of both the Langmuir and Freundlich isotherms. It is particularly valuable for describing adsorption processes on heterogeneous surfaces where the adsorption energy varies. The model's flexibility stems from the exponent β_{RP}, which allows it to transition between the Langmuir isotherm (when β_{RP}=1) and the Freundlich isotherm (when β_{RP} approaches 0). This makes it suitable for describing adsorption

on both homogeneous and heterogeneous surfaces. Unlike simpler isotherm models, the Redlich-Peterson isotherm accounts for the non-linearity of adsorption processes. This can provide a more accurate fit for experimental data, especially when the adsorption sites have varying affinities. The model is extensively used in environmental engineering, chemical engineering, and materials science for the study of adsorption phenomena. It is applied in the removal of contaminants from water, adsorption of gases on solids, and in the design of adsorption systems for industrial processes.

The parameters are usually estimated using non-linear regression techniques. Accurate estimation of these parameters is crucial for predicting the adsorption capacity and understanding the adsorption mechanism. While the Redlich-Peterson isotherm provides a good fit for a wide range of data, its complexity can be a drawback. The need for non-linear regression and the interpretation of three parameters can complicate its application compared to simpler models. In addition, the model assumes that the adsorption process does not follow a strictly Langmuir or Freundlich pattern but a combination of both. This assumption may not hold for all adsorption systems, especially those that strictly adhere to either Langmuir or Freundlich behavior. Furthermore, the Redlich-Peterson model lacks a clearly established physical basis and is thus an empirical model similar to the Sips model [70]. Hence, we will not offer a mechanical interpretation based on the best model because it is a variation of the Sips equation, which is an empirical model in and of itself.

Fritz-Schlunder III

The Fritz Schlunder III isotherm serves as a model utilized in explaining adsorption processes, on surfaces with differing properties. It blends aspects of the Langmuir and Freundlich isotherms making it applicable to scenarios where adsorption sites exhibit variations in both energy levels and capacities. This model proves to be highly effective in real world data for adsorption systems like organic pollutant adsorption on activated carbon or heavy metal removal from wastewater using biosorbents. Its capability to accommodate adsorption energies and capacities establishes it as a tool, for predicting adsorption tendencies within heterogeneous systems.

Table 3. Isothermal models' constants for the top seven models.

Model		Unit	Value	(95% confidence interval)
Unilan	q_{mU}	mg g^{-1}	16.79	-5.873 to 39.445
	b_U		2.35	0.518 to 4.178
	a_U	L mg^{-1}	0.08	0.022 to 0.129
Redlich-Peterson	K_{RP1}	L g^{1}	12.91	4.412 to 21.405
	K_{RP2}	$(mg\ L^{-1})^{-n}$	0.27	-0.044 to 0.580
	β_{RP}		0.89	0.779 to 0.999
Moreau	q_{mM}	mg g^{-1}	90.82	76.336 to 105.303
	b	L mg^{-1}	0.15	0.089 to 0.203 -0.049
	l		0.3	to 0.646
Fritz-Schlunder III	q_{mFS}	mg g^{-1}	48.24	22.653 to 73.816
	n_{FS}		0.89	0.779 to 0.999
	K_{FS}	L mg^{-1}	0.27	-0.044 to 0.580
Toth	q_{mS}	mg g^{-1}	45.93	20.956 to 70.912
	K_T	$(mg\ L^{-1})^{nT}$	4.10	-0.322 to 8.514
	n_T		0.94	0.879 to 0.998
Langmuir	q_{mL}	mg g^{-1}	81.93	76.422 to 87.440
	b_L	L mg^{-1}	0.10	0.070 to 0.133

A comparison of the SDS adsorption capacity by various adsorbents reported in the literature is presented in **Table 4**. The types of regression used in the study are also displayed and most of the studies used linear regression to analyse their data. According to Paranjape and Sadgir [71], linear regression is the most frequently used method to determine the best-fitting model for adsorption isotherms and kinetics, including the respective model parameters [5,72–75]. However, the error distribution can vary significantly depending on the linearization of the isotherm and kinetic equations, leading to either the best or worst fit. Therefore, many researchers prefer the nonlinear regression approach to verify the parameters of adsorption isotherms and kinetics. This method is based on minimizing the discrepancies between the experimental data and the predicted isotherm values.

Table 4. Summary of SDS sorption by various adsorbents.

Adsorbents	pH	Adsorbent dosage (g/L)	Maximum Adsorption capacity Q_{max} (mg/g)	Isotherm models	Kinetic models	Regression	Error function	Ref
Chemically activated coconut shell	-	2	90.9	Langmuir	PSO	Linear	R^2	[5]
Medicinal plants	5	25	-	Freundlich	PFO	Linear	R^2	[72]
Sweet lime peel charcoal	4.3	2 g	-	Langmuir	n.a.	Linear	R^2	[73]
Granular activated charcoal	7	5	3.750	Langmuir	n.a.	Linear	R^2	[74]
Waste tire rubber granules	7	5	4.164	Langmuir	n.a.	Linear	R^2	[74]
Wood charcoal	7	5	5.170	Freundlich	n.a.	Linear	R^2	[74]
Silica gel	7	5	5.181	Freundlich	n.a.	Linear	R^2	[74]
Modified cellulose	7	n.a	32.5	Langmuir	PSO	Linear	R^2	[75]
Alumina	4	n.a	230	2-step adsorption model	n.a	Non-linear	n.a	[76]

Note:
n.a. Not available
PSO Pseudo second order
PFO Pseudo first order
R^2 Coefficient of determination

CONCLUSION

Using a variety of models with one to three parameters each, the adsorption isotherm data for SDS on activated coconut shell was subjected to nonlinear regression. Moreau model outperformed Unilan, Redlich-Peterson, Fritz-Schlunder III, Toth, and Langmuir, in that order, according to statistical analysis based on error function assessments. Results from experiments were more consistent with the upper limits of adsorption capacities predicted by the Moreau and Langmuir models. The value of the maximum monolayer adsorption capacity for SDS binding to activated coconut shell according to the Langmuir's parameter q_{mL} was 81.93 mg g^{-1} (95% Confidence interval from 76.422 to 87.440), while b_L (L mg^{-1}), the Langmuir model constants was 0.10 L mg^{-1} (95% C.I. from 0.070 to 0.133). The value of the maximum monolayer adsorption capacity for SDS binding to activated coconut shell according to the Moreau's parameter q_{mM} was 90.82 mg g^{-1} (95% Confidence interval from 76.336 to 105.303), while b (L mg^{-1}), the Moreau's model constant was 0.15 L mg^{-1} (95% C.I. from 0.089 to 0.203) and l, another Moreau's dimensionless constant was 0.3 (95% C.I. from -0.049 to 0.646). These values include 95% confidence intervals, which were absent in the original work.

REFERENCES

1. Siyal AA, Shamsuddin MR, Low A, Rabat NE. A review on recent developments in the adsorption of surfactants from wastewater. J Environ Manage. 2020 Jan;254:109797.
2. Meconi GM, Ballard N, Asua JM, Zangi R. Adsorption and desorption behavior of ionic and nonionic surfactants on polymer surfaces. Soft Matter. 2016 Dec 6;12(48):9692–704.

3. Saleem J, Shahid UB, Hijab M, Mackey H, McKay G. Production and applications of activated carbons as adsorbents from olive stones. Biomass Convers Biorefinery. 2019 Dec 1;9(4):775–802.
4. Sahu RL, Dash RR, Pradhan PK. A study on adsorption of anionic surfactant from water during riverbank filtration. J Mol Liq. 2022 Aug 1;359:119247.
5. Bhandari PS, Gogate PR. Adsorptive removal of sodium dodecyl sulfate using activated coconut shell based adsorbent: Kinetic and thermodynamic study. Desalination Water Treat. 2019;165:111–23.
6. Johnson P, Trybala A, Starov V, Pinfield VJ. Effect of synthetic surfactants on the environment and the potential for substitution by biosurfactants. Adv Colloid Interface Sci. 2021 Feb 1;288:102340.
7. Azmi WNFW, Latif MT, Wahid NBA, Razak IS, Suratman S. Surfactants in runoff water at different locations in Bandar Baru Bangi, Selangor, Malaysia. Bull Environ Contam Toxicol. 2014;92(3):306–10.
8. Sini K, Idouhar M, Ahmia AC, Ferradj A, Tazerouti A. Spectrophotometric determination of anionic surfactants: optimization by response surface methodology and application to Algiers bay wastewater. Environ Monit Assess. 2017 Dec;189(12):646.
9. Ríos F, Olak-Kucharczyk M, Gmurek M, Ledakowicz S. Removal efficiency of anionic surfactants from water during UVC photolysis and advanced oxidation process in H_2O_2/UVC system. Arch Environ Prot. 2017 Jan 27;43(1):0–0.
10. Nguyen H, Phan C, Sen T. Degradation of sodium dodecyl sulphate by photoelectrochemical and electrochemical processes. Chem Eng J. 2015 Dec 1;287:633–9.
11. Arora J, Ranjan A, Chauhan A, Biswas R, Rajput VD, Sushkova S, et al. Surfactant pollution, an emerging threat to ecosystem: Approaches for effective bacterial degradation. J Appl Microbiol. 2022;133(3):1229–44.
12. Ibrahim MSS, Hashim NH. Removal of oil and grease and anionic surfactants in synthetic car wash wastewater using kapok fiber: A batch-scale study. Malays J Anal Sci. 2018 Aug 16;22(4):735–41.
13. Pal A, Pan S, Saha S. Synergistically improved adsorption of anionic surfactant and crystal violet on chitosan hydrogel beads. Chem Eng J. 2013 Feb 1;217:426–34.
14. Kowalska I. Surfactant removal from water solutions by means of ultrafiltration and ion-exchange. Desalination. 2008 Mar 1;221(1):351–7.
15. Korzenowski C, Martins M, Bernardes A, Ferreira J, Duarte E, Pinho M. Removal of anionic surfactants by nanofiltration. Desalination Water Treat. 2012 Jun 1;44:269–75.
16. Bhandari PS, Gogate PR. Kinetic and thermodynamic study of adsorptive removal of sodium dodecyl benzene sulfonate using adsorbent based on thermo-chemical activation of coconut shell. J Mol Liq. 2018;252:495–505.
17. Rehman FU. Methodological trends in preparation of activated carbon from local sources and their impacts on production: A review. Chem Int. 2018 Apr 15;4(2):109–19.
18. Ajmani A, Saranya N, Patra C, Narayanasamy S. Studies on the remediation of chromium (VI) from simulated wastewater using novel biomass of *Pinus kesiya* cone. Desalination Water Treat. 2018 Jan 1;114:192–204.
19. Rangabhashiyam S, Selvaraju N. Adsorptive remediation of hexavalent chromium from synthetic wastewater by a natural and $ZnCl_2$ activated *Sterculia guttata* shell. J Mol Liq. 2015 Jul 1;207:39–49.
20. Nakkeeran E, Saranya N, Giri Nandagopal MS, Santhiagu A, Selvaraju N. Hexavalent chromium removal from aqueous solutions by a novel powder prepared from *Colocasia esculenta* leaves. Int J Phytoremediation. 2016 Aug 2;18(8):812–21.
21. Ibisi NE, Asoluka CA. Use of agro-waste (*Musa paradisiaca* peels) as a sustainable biosorbent for toxic metal ions removal from contaminated water. Chem Int. 2018;4(1):52–9.
22. Motulsky HJ, Ransnas LA. Fitting curves to data using nonlinear regression: a practical and nonmathematical review. FASEB J. 1987;1(5):365–74.
23. Tawfik GM, Dila KAS, Mohamed MYF, Tam DNH, Kien ND, Ahmed AM, et al. A step by step guide for conducting a systematic review and meta-analysis with simulation data. Trop Med Health. 2019 Aug 1;47(1):46.
24. Khare KS, Phelan FR. Quantitative Comparison of Atomistic Simulations with Experiment for a Cross-Linked Epoxy: A Specific Volume-Cooling Rate Analysis. Macromolecules. 2018;51(2):564–75.
25. Ridha FN, Webley PA. Anomalous Henry's law behavior of nitrogen and carbon dioxide adsorption on alkali-exchanged chabazite zeolites. Sep Purif Technol. 2009;67(3):336–43.
26. Langmuir I. THE ADSORPTION OF GASES ON PLANE SURFACES OF GLASS, MICA AND PLATINUM. J Am Chem Soc. 1918;40(2):1361–402.
27. Jovanović DS. Physical adsorption of gases - I: Isotherms for monolayer and multilayer adsorption. Kolloid-Z Amp Z Für Polym. 1969;235(1):1203–13.
28. Carmo AM, Hundal LS, Thompson ML. Sorption of hydrophobic organic compounds by soil materials: Application of unit equivalent Freundlich coefficients. Environ Sci Technol. 2000;34(20):4363–9.
29. Radushkevich LV. Potential theory of sorption and structure of carbons. Zhurnal Fiz Khimii. 1949;23:1410–20.
30. Dubinin MM. Modern state of the theory of volume filling of micropore adsorbents during adsorption of gases and steams on carbon adsorbents. Zh Fiz Khim. 1965;39(6):1305–17.
31. Mahanty B, Behera SK, Sahoo NK. Misinterpretation of Dubinin–Radushkevich isotherm and its implications on adsorption parameter estimates. Sep Sci Technol. 2023 May 3;58(7):1275–82.
32. Mudhoo A, Pittman CU. The Dubinin-Radushkevich models: Dissecting the *ps*/*p* to *cs*/*c*e replacement in solid-aqueous interfacial adsorption and tracking the validity of E = 8 kJ mol–1 for assigning sorption type. Chem Eng Res Des. 2023 Oct 1;198:370–402.
33. Temkin MI, Pyzhev V. Kinetics of ammonia synthesis on promoted iron catalysts. Acta Physicochim USSR. 1940;12(3):327–56.
34. Chu KH. Revisiting the Temkin Isotherm: Dimensional Inconsistency and Approximate Forms. Ind Eng Chem Res [Internet]. 2021 Aug 16 [cited 2022 Sep 1]; Available from: https://pubs.acs.org/doi/pdf/10.1021/acs.iecr.1c01788
35. Redlich O, Peterson DL. A Useful Adsorption Isotherm. Shell Dev Co Emeryv Calif. 1958;63:1024.
36. Sips R. On the structure of a catalyst surface. J Chem Phys. 1948;16(5):490–5.
37. Tóth J. Uniform interpretation of gas/solid adsorption. Adv Colloid Interface Sci. 1995;55(C):1–239.
38. Hill AV. The possible effects of the aggregation of the molecules of haemoglobin on its dissociation curves. J Physiol. 1910;40:iv–vii.
39. Khan AA, Singh RP. Adsorption thermodynamics of carbofuran on Sn (IV) arsenosilicate in H+, Na+ and Ca2+ forms. Colloids Surf. 1987;24(1):33–42.
40. Brunauer S, Emmett PH, Teller E. Adsorption of Gases in Multimolecular Layers. J Am Chem Soc. 1938;60(2):309–19.
41. Vieth WR, Sladek KJ. A model for diffusion in a glassy polymer. J Colloid Sci. 1965;20(9):1014–33.
42. Radke CJ, Prausnitz JM. Adsorption of Organic Solutes from Dilute Aqueous Solution of Activated Carbon. J Am Chem Soc. 1972;11(4):445–51.
43. Liu Y, Liu YJ. Biosorption isotherms, kinetics and thermodynamics. Sep Purif Technol. 2008;61(3):229–42.
44. Tran HN, Bollinger JC, Lima EC, Juang RS. How to avoid mistakes in treating adsorption isotherm data (liquid and solid phases): Some comments about correctly using Radke-Prausnitz nonlinear model and Langmuir equilibrium constant. J Environ Manage. 2023 Jan 1;325(Pt A):116475.
45. Brouers F, Sotolongo O, Marquez F, Pirard JP. Microporous and heterogeneous surface adsorption isotherms arising from Levy distributions. Phys Stat Mech Its Appl. 2005 Apr 1;349(1):271–82.
46. Hamissa AMB, Brouers F, Mahjoub B, Seffen M. Adsorption of Textile Dyes Using Agave Americana (L.) Fibres: Equilibrium and Kinetics Modelling. Adsorpt Sci Technol. 2007 Jun 1;25(5):311–25.
47. Fritz W, Schluender EU. Simultaneous adsorption equilibria of organic solutes in dilute aqueous solutions on activated carbon. Chem Eng Sci. 1974;29(5):1279–82.
48. Chu KH, Tan B. Is the Frumkin (Fowler–Guggenheim) adsorption isotherm a two- or three-parameter equation? Colloid Interface Sci Commun. 2021 Nov 1;45:100519.
49. Martucci A, Braschi I, Bisio C, Sarti E, Rodeghero E, Bagatin R, et al. Influence of water on the retention of methyl tertiary-butyl ether by high silica ZSM-5 and Y zeolites: A multidisciplinary study on the adsorption from liquid and gas phase. RSC Adv. 2015;5(106):86997–7006.

50. Baudu M. Etude des interactions solute–fibres de charbon actif. Application et regeneration. Universite de Rennes I; 1990.
51. Parker Jr. GR. Optimum isotherm equation and thermodynamic interpretation for aqueous 1,1,2-trichloroethene adsorption isotherms on three adsorbents. Adsorption. 1995;1(2):113–32.
52. van Vliet BM, Weber Jr WJ, Hozumi H. Modeling and prediction of specific compound adsorption by activated carbon and synthetic adsorbents. Water Res. 1980;14(12):1719–28.
53. Burnham KP, Anderson DR. Multimodel inference: Understanding AIC and BIC in model selection. Sociol Methods Res. 2004;33(2):261–304.
54. Akaike H. A New Look at the Statistical Model Identification. IEEE Trans Autom Control. 1974;19(6):716–23.
55. Dan-Iya BI, Shukor MY. Isothermal Modelling of the Adsorption of Chromium onto Calcium Alginate Nanoparticles. J Environ Microbiol Toxicol. 2021;9(2):1–7.
56. Marquardt DW. An Algorithm for Least-Squares Estimation of Nonlinear Parameters. J Soc Ind Appl Math. 1963;11(2):431–41.
57. Seidel A, Gelbin D. On applying the ideal adsorbed solution theory to multicomponent adsorption equilibria of dissolved organic components on activated carbon. Chem Eng Sci. 1988 Jan 1;43(1):79–88.
58. Porter JF, McKay G, Choy KH. The prediction of sorption from a binary mixture of acidic dyes using single- and mixed-isotherm variants of the ideal adsorbed solute theory. Chem Eng Sci. 1999;54(24):5863–85.
59. Gritti F, Guiochon G. Retention of Ionizable Compounds in Reversed-Phase Liquid Chromatography. Effect of the Ionic Strength of the Mobile Phase and the Nature of the Salts Used on the Overloading Behavior. Anal Chem. 2004 Aug 1;76(16):4779–89.
60. Ruthven DM. Principles of Adsorption and Adsorption Processes. John Wiley & Sons; 1984. 466 p.
61. Wang Z, Marcus RK. Roles of interstitial fraction and load conditions on the dynamic binding capacity of proteins on capillary-channeled polymer fiber columns. Biotechnol Prog. 2015;31(1):97–109.
62. Valenzuela DP, Myers AL. Adsorption equilibrium data handbook. Englewood Cliffs, N.J: Prentice Hall; 1989. 366 p.
63. McKay G, Mesdaghinia A, Nasseri S, Hadi M, Solaimany Aminabad M. Optimum isotherms of dyes sorption by activated carbon: Fractional theoretical capacity & error analysis. Chem Eng J. 2014;251:236–47.
64. Langmuir I. The constitution and fundamental properties of solids and liquids. Part I. Solids. J Am Chem Soc. 1916;38(11):2221–95.
65. Foo KY, Hameed BH. Insights into the modeling of adsorption isotherm systems. Chem Eng J. 2010;156(1):2–10.
66. Wu Z, Joo H, Ahn IS, Haam S, Kim JH, Lee K. Organic dye adsorption on mesoporous hybrid gels. Chem Eng J. 2004 Sep 15;102(3):277–82.
67. Chern JM, Wu CY. Desorption of dye from activated carbon beds: Effects of temperature, pH, and alcohol. Water Res. 2002 Jan 1;35:4159–65.
68. Pimentel CH, Díaz-Fernández L, Gómez-Díaz D, Freire MS, González-Álvarez J. Separation of CO2 using biochar and KOH and ZnCl2 activated carbons derived from pine sawdust. J Environ Chem Eng. 2023;11(6).
69. Chen R, Liu J, Dai X. Adsorption equilibrium of ammonia and water on porous adsorbents at low pressure: Machine learning-based models. J Clean Prod. 2022;378.
70. Chu KH, Hashim M, Santos YTDC, Debord J, Harel M, Bollinger JC. The Redlich–Peterson isotherm for aqueous phase adsorption: Pitfalls in data analysis and interpretation. Chem Eng Sci. 2023 Nov 28;285:119573.
71. Paranjape P, Sadgir P. Linear and nonlinear regression methods for isotherm and kinetic modelling of iron ions bioadsorption using Ocimum sanctum Linn. leaves from aqueous solution. Water Pract Technol. 2023 Jul 18;18(8):1807–27.
72. Tomar P, Verma C, Sar SK. Medicinal plants the key bio-adsorbents for anionic surfactant (SDS) from waste water. Chem Process Eng Res. 2013;15:57–65.
73. Nagwanshi JK, Agrawal MA. Efficiency of treated agricultural adsorbent during recycling of waste water for removal of SDS. Res J Pharm Technol. 2018 Jul 31;11(7):3018–22.
74. Purakayastha PD, Pal A, Bandyopadhyay M. Adsorbent selection for anionic surfactant removal from water. Indian J Chem Technol. 2005;12:281–4.
75. Zou M, Zhang H, Miyamoto N, Kano N, Okawa H. Adsorption of an anionic surfactant (sodium dodecyl sulfate) from an aqueous solution by modified cellulose with quaternary ammonium. Polymers. 2022 Apr 5;14(7):1473.
76. Nguyen TMT, Do TPT, Hoang TS, Nguyen NV, Pham HD, Nguyen TD, et al. Adsorption of Anionic Surfactants onto Alumina: Characteristics, Mechanisms, and Application for Heavy Metal Removal. Int J Polym Sci. 2018 Dec 13;2018:e2830286.